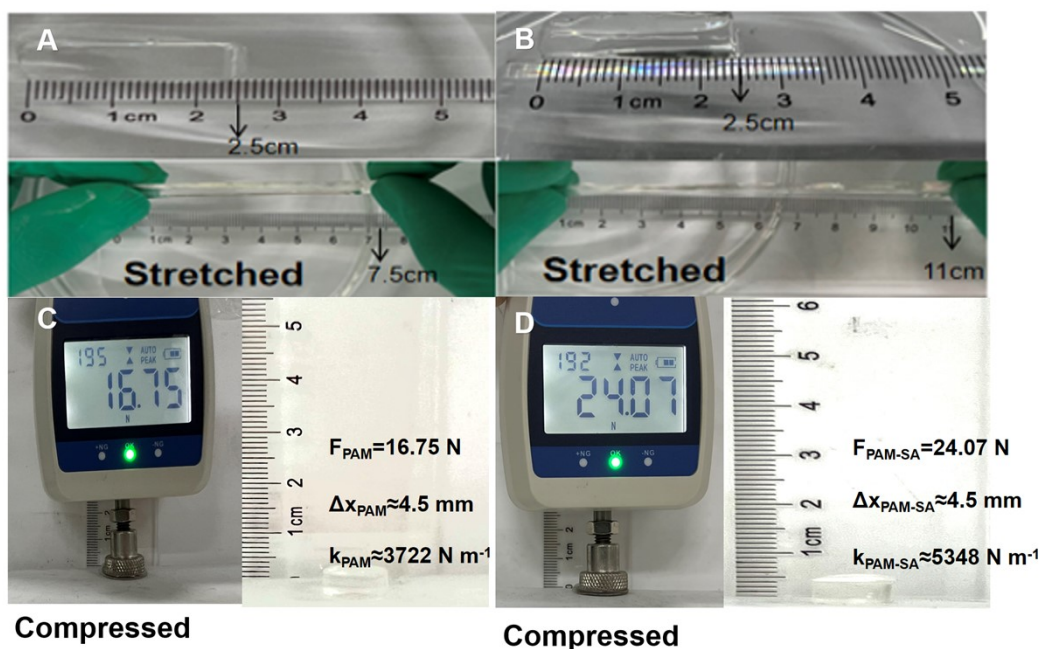


9

10 **Figure S1. Characterization of Hydrogels.** (A-D) SEM images of these hydrogels with different
 11 magnifications. resulting in the formation of a lamellar double network structure. (E) FT-IR of
 12 PAM-SA and PAM hydrogel. In PAM samples, the peak at 3343 and 3201 cm^{-1} corresponded to
 13 the stretching vibrations of the amino group $-\text{NH}_2$. The peak at 1648 cm^{-1} was attributed to the
 14 carbonyl $\text{C}=\text{O}$ stretching band, while the peak at 1602 cm^{-1} corresponded to the amino group $-\text{NH}_2$.
 15 However, in PAM-SA samples, the stretching of $-\text{NH}_2$ group was shifted to 1611 and 1674 cm^{-1} ,
 16 and N-H stretching peaks at 3343 and 3201 cm^{-1} were shifted to 3340 and 3186 cm^{-1} , respectively.
 17 Additionally, the stretching of carbonyl $\text{C}=\text{O}$ was shifted from 1648 cm^{-1} (PAM) to 1647 cm^{-1}
 18 (PAM-SA hydrogel). (F) Swelling properties of PAM-SA and PAM.

19



20

21 **Figure S2. Characterization of Toughness of Hydrogels.** (A) Tensile properties of PAM. (B)
 22 Tensile properties of PAM-SA. (C) Compression performance of PAM. (D) Compression
 23 performance of PAM-SA.

24

25 **Movie S1.** This movie shows the detailed process of electric field reconstruction for
 26 the wound site